ON-BOARD ENGINE LIFE USAGE MONITORING BY REAL TIME COMPUTATION

* Manfred Koehl

Abstract : Aero engine components are subject to considerable mechanical and thermal loads. Some extremely stressed engine parts can reach their life limits within the engine service time. Life usage monitoring activities serve to identify the proper time for their replacement. Only by a fleet wide individual monitoring of each critical area in each engine, an optimal exploitation of the released life can be achieved, since the actually measured engine parameters are used to determine the current state of the remaining life. The monitoring procedures consist of effective algorithms for use in real time, which allow for fast calculation of the temperatures and stresses from the input signals as they appear under real aircraft and engine manoeuvring. Damage results are available immediately after the end of a flight. The present contribution is concerned with the algorithms of on-board life usage monitoring software with respect to two lifing concepts, the safe crack initiation and the safe crack propagation life concept. The crack initiation concept declares a structural part's life as exhausted if a small crack of a predefined depth has been initiated with a given probability. The life limit according to the crack popagation concept is equal to a certain percentage of the dysfunction life (e.g. the onset of unstable crack growth). Applicability of the methods is underlined by results obtained with OLMOS - the on-board life usage monitoring system of the German Air Force Tornado fleet.

INTRODUCTION

Those aero engine components where highly stressed areas are located and a failure could jeopardise the flight safety, are declared as fracture critical parts and released only for limited life. In case their life limits are reached within the service time of the engine, they must be replaced. Life usage monitoring activities serve to identify the proper time. How long a critical part can be kept in service depends on both the released life at the critical areas and their life consumption due to operational usage.
The life consumed during an engine run or flight is based on stresses and temperatures at the critical areas of the components. These parameters depend on the actual flight mission profiles, engine intake conditions, individual pilot reactions and many other influences. Life usage monitoring enables to calculate the life consumption of each critical part individually using actually measured engine parameters. Thus, the best exploitation of the released life is only achievable by individual monitoring rather than, for example, by estimating the life consumption on the basis of average values per flight time.

* MTU Aero Engines GmbH, Dept. TPM, 80976 Muenchen, Germany

Two lifing concepts are considered, the safe crack initiation concept and the safe crack propagation concept. While the safe crack initiation life is established as the number of reference stress cycles (most damaging cycle of the design mission) to reach an accepted statistical probability for the existence of a crack with a depth of 0.4 mm, the safe crack propagation life is established as 2/3 of the number of reference cycles to reach an accepted statistical probability for the presence of the dysfunction condition (e.g. the onset of unstable crack growth). The statistical probability takes into account that material strength and crack growth properties exhibit some scatter. For the weakest individual of the part's population, the structural integrity must be ensured. Generally accepted statistical probabilities for that weakest part are in the range of 1 out of 750 to 1 out of 1000. It is expected that the crack propagation life could partly be utilised to extend the usage period beyond the limits set by the safe crack initiation life concept, as sketched in Figure 2.
Components treated under either of these lifing concepts are not inspected for cracks when they are retired. Re-use of the parts beyond the safe crack initiation respectively propagation life is not considered, although most of the parts will not contain a crack grown to the depth which is correlated with the respective criterion.
Note that the safe crack initiation life concept cannot provide a measure for the real safety of the critical part, since it is unable to predict a value for the failure margin. In most of the applications there will be sufficient margin for a crack to grow to part dysfunction, but it is also possible that the dysfunction life is very close to the crack initiation life. As an example, this was suspected to be the cause for an uncontained engine failure that occurred at Philadelphia, Pennsylvania, on September 22, 2000, as result of cracking and rupture of a high pressure turbine disk in a General Electric CF6-80C2B2 engine [1]. In such very rare cases the crack initiation life cannot be considered as really safe, in contrast to the safe crack propagation life where a safety margin is defined.
The present contribution is concerned with the algorithms of on-board life usage monitoring software with respect to both the crack initiation and the crack propagation life concept. Applicability of the methods is underlined by results obtained with OLMOS - the on-board life usage monitoring system of the German Airforce Tornado fleet. This system has been in use since 1987 and was improved in the following years by periodical updates according to the newest developments. One of the latest improvements was the extension to crack propagation monitoring, applied to critical areas in a compressor disc and in the rim region of a turbine disc.

ON-BOARD LIFE MONITORING IN REAL TIME

The procedures for individual monitoring consist of effective algorithms for use in real time, able to compute the consumed life of a critical area directly from measured engine signals such as spool speeds, intake conditions and, if available, gas path temperatures and pressures. The algorithms allow for fast calculation of the temperatures and stresses from the input signals, as they appear under real aircraft and engine manoeuvring. Damage results are available immediately after the end of a flight. Life consumption is measured in damage related physical or technical units. Normally, the most damaging cycle of the design mission is declared as the reference cycle for the considered critical area and used as the unit for damage.
Details of the method have been published at several occasions [2-7]. Here only a summary is given. The method determines the thermal and mechanical boundary conditions for the engine components on the basis of measured time histories of engine operating

parameters (such as spool speeds, engine intake conditions and gas path temperatures). Based on these boundary conditions, the transient temperature development within the components is calculated. Stresses at critical areas are computed, which are then used together with the corresponding temperature histories to predict the related damage. Critical area damage is accumulated over all engine runs, so to build up complete life consumption records for all monitored parts of an engine. In Figure 1 the monitoring scheme is illustrated.

For most of the critical areas, the concept of safe crack initiation life is employed. Under this concept, the number of reference cycles needs to be predicted, which the critical area can undergo until a fatigue crack will have been generated and grown to the predicted depth of 0.4 mm. Material *SN*-curves are used which describe the relationship between applied stress range and the corresponding number of cycles to crack initiation. Mean stress and temperature effects are covered as well.

For critical areas where the original safe crack initiation life is extended into the safe crack growth regime, additionally the safe crack propagation life needs to be predicted. For this prediction, typically the methods of linear elastic fracture mechanics are used to create a data base for crack propagation monitoring. Two things are required, namely the stress intensity factor range of the most damaging cycle accompanied by *R*-ratio (stress intensity factor ratio of cycle minimum to cycle maximum value) and temperature, and the crack propagation law relevant for the used material. The crack propagation law describes the crack propagation rate as function of the stress intensity factor range, considering also *R*-ratio and temperature. The accumulating crack growth process is simulated by integration of the crack propagation rate from the initial crack depth to the onset of instability under reference cycle loading. From the number of cycles necessary to propagate the crack up to the dysfunction criterion, one can derive the safe crack propagation life.

TEMPERATURE AND STRESS CALCULATION

Monitored are the stresses in those areas of the engine structure which were found to be life limiting for the respective component by the finite element design analyses. The temperatures have to be calculated also in some additional structure points. These points are selected in such a way that a good approximation of the thermal stresses at the critical areas is possible, and they must be dense enough to allow for an adequate modelling of the heat conduction.

In a first step, the relevant heat sources (gas path or cooling air temperatures) must be available. They are either measured, if possible, or - based on performance design calculations - modelled. In many cases it turned out that a model of the form of a power function $T_{gas}^{*} = a + b \cdot (N_{rot}^{*})^{c}$ is sufficient, where T_{gas}^{*} and N_{rot}^{*} are the thermodynamically reduced gas temperature and rotational speed (normalized to ISA standard conditions). The parameters *a, b* and *c* are fitted according to the individual gas temperature of the design calculation.

The metal temperature development requires a dynamical model. The temperatures are calculated successively in small time steps (for example steps of 0.5s), starting with an initial temperature distribution. The temperature at time step *i* follows from its value at the previous time step *i-1* in the following way. To every considered temperature point a leading temperature is assigned which depends on the gas temperature T_{gas}:

$$T_{lead}^{(i)} = T_{lead}^{(i-1)} + a \cdot (b \cdot T_{gas}^{(i)} - T_{lead}^{(i-1)}) \qquad (1)$$

This leading temperature T_{lead} and the temperatures of (normally three or four) neighbouring points T_j determine the increment of the metal temperature of the considered point:

$$T^{(i)} = T^{(i-1)} + c \cdot (T_{lead}^{(i)} - T^{(i-1)}) + \sum d_j \cdot (T_j^{(i-1)} - T^{(i-1)}) \quad (2)$$

The second term on the right hand side represents the heat transfer from gas, the third term the heat conduction in the metal. The parameters a, c, d_j are functions of the rotational speed N_{rot} , for example represented as power functions of the form $e + f \cdot (N_{rot} / N_{rot,ref})^{g}$ with a given reference speed $N_{rot,ref}$ and constants e, f and g. The values of these constants are determined by using the results of the design mission FE-analysis in such a way that the maximum temperature error between the model-calculation and the FE-calculation is minimized, taken over the whole design mission. The parameter b is also dependent on the rotational speed. It is calculated for about five selected speed values under the condition that the steady state metal temperatures for these speeds - which are known from FE-calculations - are met. The b-values for other speeds are linearly interpolated.
The stresses for each critical area are modelled as the sum of assembly-, centrifugal-, and thermal-stresses:

$$\sigma = c_0 + c_{cf} \cdot N_{rot}^2 + \sum c_j \cdot T_j \quad (3)$$

The thermal stresse are approximated as a linear combination of the temperature in some representative points. The constants c_0 , c_{cf} and c_j are optimized by minimizing the maximum stress error over the whole design mission compared with the FE-calculation.

DATA BASE FOR CRACK PROPAGATION MONITORING

It is the aim of this section to introduce a procedure for the creation of a data base for an individual critical area which enables the real time calculation of the stress intensity factor as a function of the stress $\sigma_{critical\ area}$ and of a crack depth parameter a :

$$K(a) = f(\sigma_{critical\ area} , a) \quad (4)$$

The stress $\sigma_{critical\ area}$ is the elastic stress at the critical area of the uncracked structure. This stress is calculated by the above introduced monitoring algorithms. The crack depth parameter a itself is not known, but for given reference conditions and a given initial crack depth, there exists a direct correlation between the monitored accumulated number of applied cycles N and the crack depth a (to be obtained by integration of the crack propagation law).
For a given load cycle the stress intensity factor determines the amount of crack growth, the so called crack growth rate da/dN. The stress intensity factor depends on the geometry of the component, on the stress field around the critical area, and on the current shape of the crack. As these quantities in aero engine components are very complex, text book solutions for the stress intensity factors are generally not available. Thus, they are calculated by finite element analyses.
A 3D finite element model is used, where the crack surface and the crack front are introduced. As an example, a modelled crack front at a critical area in the rim slot fillet of a turbine disc is shown in Figure 3. An automated procedure has been established which allows to simulate the development of the crack using finite element calculations in combination with an appropriate crack growth law. Details of this technique were already pub-

lished in numerous articles, e.g. [8] (a comprehensive list of these publications can be found on the web homepage [9]). The load case belonging to the maximum stress of the reference cycle is used. All relevant loads - as centrifugal and thermal loads - contributing to the stress field around the critical area are included.
Now, one can choose a path at the analysed crack surface from the point where the crack has originated (the critical area) into the depth of the considered structure, as shown in Figure 4. Along this path the crack depth a is measured. For the path, a relationship between the crack depth a and the corresponding stress intensity factor $K(a)$ can be established. Dividing the stress intensity factor by the monitored stress $\sigma_{critical\ area} = \sigma(0)$ present at the uncracked critical area at $a=0$ itself, defines a so called geometry function $g(a)$. This geometry function provides the relationship between the stress at the critical area and the stress intensity factor at the crack front for each value of the crack depth a and enables us to calculate the time history of the stress intensity factor from the time history of the stress at the critical area including the effect of increasing crack depth.
For this procedure it is assumed that the stress fields around the critical area are proportional for all load cases of the mission. In fact, this is not the case. But the error is considered negligible as long as the stress intensity factors for the higher stress levels are modelled correctly. Deviations for sub-cycle stress intensity factor ranges are acceptable as their contribution to the overall damage is small.
Currently only a correction for residual stresses is made. The basic idea for this correction is that during the first load cycles some local plastification occurs, what causes some redistribution of the stress fields, as illustrated in Figure 4. After initial plastification, the component is assumed to behave linearly, so that the application of linear elastic fracture mechanics methods appear adequate. This redistribution is accounted for by an additional additive term $K_{add}(a)$ in the formula for the stress intensity factor.
Now we can put the expression (4) in a more concrete form :

$$K(a) \quad = \quad g(a) \cdot \sigma_{critical\ area} \quad + \quad K_{add}(a) \tag{5}$$

The geometry function $g(a)$ and the additional additive term $K_{add}(a)$ as a function of the crack depth a are determined by finite element analyses as follows:
Firstly, a 3D finite element analysis of the uncracked structure under *reference load conditions* is performed, linear-elastically as well as elastic-plastically, in order to determine the linear-elastic stress $\sigma_{elastic,ref}(a)$ and the elastic-plastic stress $\sigma_{elastic\text{-}plastic,ref}(a)$ along the predefined crack path a.
Secondly, a couple of linear-elastic 3D finite element analyses of the structure containing cracks of different depths according to Figure 4 is performed *under reference load conditions*), yielding the stress intensity factor $K^*_{ref}(a)$ as a function of the chosen crack path a .
Using the results of these analyses yields according to [10]:

$$g(a) \ := \quad K^*_{ref}(a) \ / \ \sigma_{elastic,ref}(0) \tag{6}$$

$$K_{add}(a) \ := \quad K^*_{ref}(a) \cdot \ (\ \sigma_{elastic\text{-}plastic,ref}(a) - \sigma_{elastic,ref}(a) \ ) \ / \ \sigma_{elastic,ref}(a) \tag{7}$$

For application in the monitoring system the quantities g and K_{add} as a function of a or N are stored in a table as sketched in Figure 4. Additionally, the crack growth rate $(da/dN)_{ref}$ for reference load is listed in the table. It is needed for the relative damage calculation (next section). Figure 4 also shows a graph of g and K_{add} as functions of a. The geometry function g increases usually monotonically with the depth a. The additive correction K_{add} starts with a negative value at the critical area ($a=0$), increases with increasing depth a,

and becomes slightly positive. This behaviour of $K_{add}(a)$ is caused by a stress redistribution after plastification as also illustrated by the graph on the left in Figure 4. In the chosen example, the highest plastification occurs at the critical area ($a=0$), reducing the stress intensity factor, while - as a static balance - in deeper, not plastified regions the level is greater compared to purely elastic results.

DAMAGE CALCULATION

In life usage monitoring the released life of an engine component is formulated in terms of the maximum allowed number of reference cycles. Therefore, it is convenient to define the relative cyclic damage of an arbitrarily given stress cycle by the ratio of the damage of the cycle to the damage due to one reference cycle : D_{cycle} *: = (damage of cycle) / (damage of reference cycle).* Thus, the relative cyclic damage is expressed in units of *one reference cycle.* Application of this definition leads to different expressions for the crack initiation and for the crack propagation regime.

If N_{cycle} denotes the total number of a given stress cycle leading to crack initiation, a measure for the damage due to one cycle is introduced by its inverse $1/N_{cycle}$. In particular, the damage of one reference cycle is denoted by $1/N_{ref}$. The relative cyclic damage for the crack initiation phase therefore is $D_{cycle} = N_{ref} / N_{cycle}$. For the crack propagation phase, the damage of an arbitrary cycle can be quantified by the crack propagation rate $(da/dN)_{cycle}$, the damage of the reference cycle by $(da/dN)_{ref}$, yielding the relative cyclic damage $D_{cycle} = (da/dN)_{cycle} / (da/dN)_{ref}$.

Under the concept of crack initiation life, the damage accumulation process is assumed to be a linear process. The damage increments are independent from the current state of accumulated damage and the Miner's Rule is used, i.e. the relative cyclic damage values of each extracted cycle are added up.

The damage accumulation process in the crack propagation regime - in contrast - is a non-linear one. The damage increment depends additionally on the currently accumulated stage of damage. The physical representation of the accumulated damage is the crack depth a, but in the terminology of life usage the number of consumed reference cycles N is used. The current stage of damage determines on one hand the value of the geometry function $g(a)$ and the term $K_{add}(a)$ representing the residual stress (see above in equations (6), (7)), and on the other hand the crack growth increment of the reference cycle $(da/dN)_{ref}$ which is used as reference for the relative cyclic damage.

If the concept of safe crack propagation life is used to extend the life beyond the safe crack initiation life, then it is necessary that the algorithm switches from one procedure to the other controlled by the current stage of cumulated damage. To distinguish between both procedures, it is checked if the already consumed number of cycles is below or above the released number of cycles to crack initiation. If it is below, then the crack initiation damage process applies, otherwise the crack propagation process.

The life usage monitoring process for aero engines is strongly related to the history of an engine run [2]. Each engine run is treated separately and at its end all cycles are closed and the damage accounts are updated. Since an engine run can be considered as short compared to the life of fracture critical parts and the cracks at critical areas grow slowly, we can assume that the current state of damage is nearly constant during one engine run. Therefore it is justified to determine the values of the crack propagation damage dependent parameters only at the beginning of each engine run and keep them constant for all cycles of this run. These parameters, the geometry function $g(a)$, the term $K_{add}(a)$**,** and the

reference cycle crack propagation increment $(da/dN)_{ref}$, are given as functions of the accumulated number of cycles. Usually a representation in form of tables according to Figure 4 is used where the current values are obtained by linear interpolation.
The procedure of the flight damage calculation (more precise: of the damage calculation for an entire engine run) for crack intiation and propagation is sketched in Figure 5.
For crack initiation, the extracted stress cycles are converted into equivalent zero-max-cycles, and their damage $1/N_{cycle}$ is determined by use of the S-N diagram. The total damage of the flight expressed in multiples of reference cycles is obtained by summation over the relative cyclic damage values $D_{cycle} = N_{ref} / N_{cycle}$ of each cycle.
For crack propagation, all extracted stress cycles are converted into stress intensity factor cycles using the geometry function $g(a)$ and the term $K_{add}(a)$. The corresponding crack propagation increments $(da/dN)_{cycle}$ are calculated by evaluation of the crack propagation law according to stress intensity factor range ΔK , R-ratio and temperature. Dividing the respective crack propagation increments $(da/dN)_{cycle}$ by the reference cycle crack propagation $(da/dN)_{ref}$ yields the damage increment $D_{cycle} = (da/dN)_{cycle} / (da/dN)_{ref}$ of the considered cycle in terms of multiples of the reference cycle. Damage increments are accumulated over the whole engine run.
In the final calculation phase - i.e. after the engine has been switched off - the damage accumulated over this engine run is added to the damage accounts.

EXAMPLE FOR LIFE EXTENSION BY MONITORING THE CRACK PROPAGATION LIFE

In the German OLMOS system of the TORNADO engine RB199 the concepts of crack initiation and crack propagation life are combined, where the safe crack propagation life is used to extend the initially released crack initiation life.
The cyclic damage accumulated over all cycles and subcycles of an individual flight can be expected to be higher in the crack propagation regime than in the crack initiation phase because of the different effect of the subcycles. The subcycle damage in the crack propagation regime is higher due to different slopes of SN-curve and crack propagation law, and more damaging subcycles exist in the crack propagation regime since the crack propagation threshold is relatively lower than the endurance limit in the crack initiation phase. Therefore, the ratio of cyclic damage of crack initiation to crack propagation might strongly depend on the flight profile. Considering these effects, one may expect higher scatter in flight to flight damage for the crack propagation phase.
A main frame computer simulation of the damage calculation procedure described in the previous section was applied to the critical area in the rim slot fillet of a turbine disc according to Figure 3 for a representative number of recorded real flight missions. It turned out that scatter reaches from nearly 1 (for flights with virtually no subcycle damage) to about 3.5 (for flights with a significant number of damaging subcycles). This clearly demonstrates that there does not exist a fixed ratio between crack propagation and crack initiation damage, but that this ratio is significantly influenced by operational usage profiles. As a result, for the crack propagation the average damage per flight was found to be greater by a factor between 1.5 and 2.0 compared with the crack initiation. This effect was expected.
Finally, the question on the benefit gained by the introduction of the safe crack propagation life concept can be treated by comparing the crack initiation life consumption with the crack propagation life consumption over a representative number of flight missions.

To quantify the benefit due to the extension of the safe crack initiation life concept to the safe crack propagation life, we refer to the 2/3 dysfunction life which is equal to 2/3 of the number of reference cycles up to the dysfunction criterion (e.g. unstable crack growth), including crack initiation and propagation phase. If we refer the numbers of reference cycles in the crack initiation phase and those in the crack propagation phase to the respective damage per flight time, the respective life times are obtained. Thus, we are able to compare the flight time in the crack propagation phase with the flight time in the crack initiation phase. The ratio yields a measure for the benefit gained by the inclusion of the crack propagation regime.
For the example shown in Figure 3 (rim slot fillet of a turbine disc) the service period in terms of engine flight time can be increased by about 40%, if in addition to the crack initiation regime a safe percentage of the crack propagation regime is utilised.

REFERENCES

[1] National Transportation Safety Board, Washington, D.C. 20594, NTSB Safety Recommendation A-00-121 through -124, December 12,2000.

[2] Broede, J. 1988. "Engine Life Consumption Monitoring Program for RB199 Integrated in the On-Board Life Monitoring System", AGARD CP 448, Quebec 1988, Paper 9.

[3] Broede, J. and H. Pfoertner. 1989. "Advanced Algorithm Design and Implementation in On-Board Microprocessor Systems for Engine Life Usage Monitoring", 15th Symposium AIMS, Aachen 1989, DLR-Mitt. 90-04,1990.

[4] Pfoertner, H. and C. Roß. 1995. "Preparing Life Usage Monitoring for the Next Decade", 18th International Symposium AIMS, Stuttgart 1995.

[5] Broede, J. and H. Pfoertner. 1997. "OLMOS in GAF MRCA Tornado - 10 Years of Experience with On-Board Life Usage Monitoring", 33rd AIAA/ASME/SAE/ASEE Joint Propulsion Conference & Exhibit, Seattle, WA 1997.

[6] Broede, J. 2001. "Saving Costs in Design, Manufacturing and Operation of Aero Engine Parts", 8th CEAS European Propulsion Forum, Affordability and the Environment, Key Challenges for Propulsion in the 21st Century, 26-28 March 2001, Nottingham, UK.

[7] Pfoertner, H. 2001. "Extension of the Usable Engine Life by Modelling and Monitoring", RTO Lecture Series 218bis, "Aging Aircraft Fleets: Structural and Other Subsystem Aspects", in Sofia (Bulgaria), RTO-EN-015, March 2001.

[8] Dhondt., G. 1998. "Automatic Three-Dimensional Cyclic Crack Propagation Predictions with Finite Elements at the Design Stage of an Aircraft Engine", Proceedings of the "Applied Vehicle Technology Panel Symposium on Design Principles and Methods For Aircraft Gas Turbine Engines" of the RTO, Toulouse, France, 11-15 May 1998, Paper 33.

[9] Dhondt,G. Homepage entitled The Numerical Fracture Mechanics Corner. http://home.t-online.de/home/dhondt/

[10] Broede, J. and M. Köhl. 1999. "Aero Engine Life Usage Monitoring Including Safe Crack Propagation", Proceedings of the 2nd International Workshop on Structural

Health Monitoring, Stanford University, Stanford, CA, September 8-10, 1999.

FIGURES

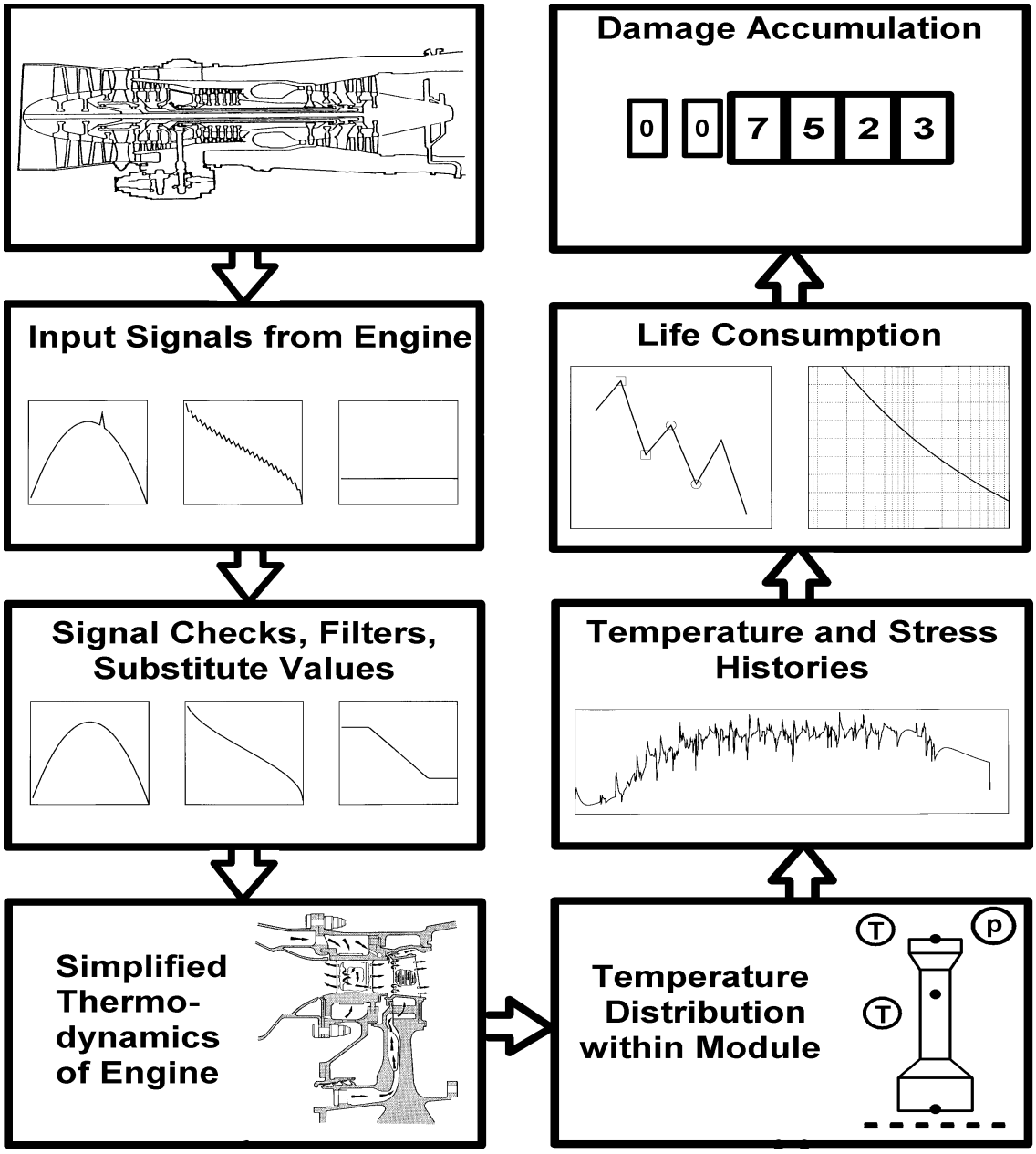

FIGURE 1 : REAL TIME MONITORING SCHEME

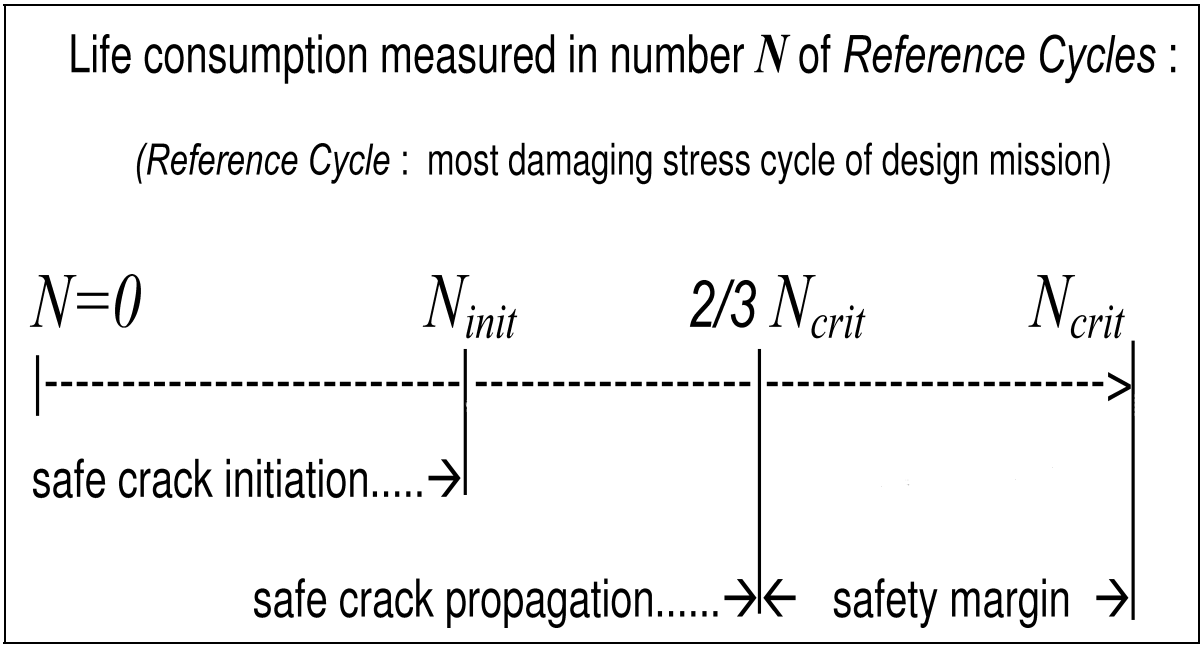

FIGURE 2 : LIFE CONSUMPTION SCHEME

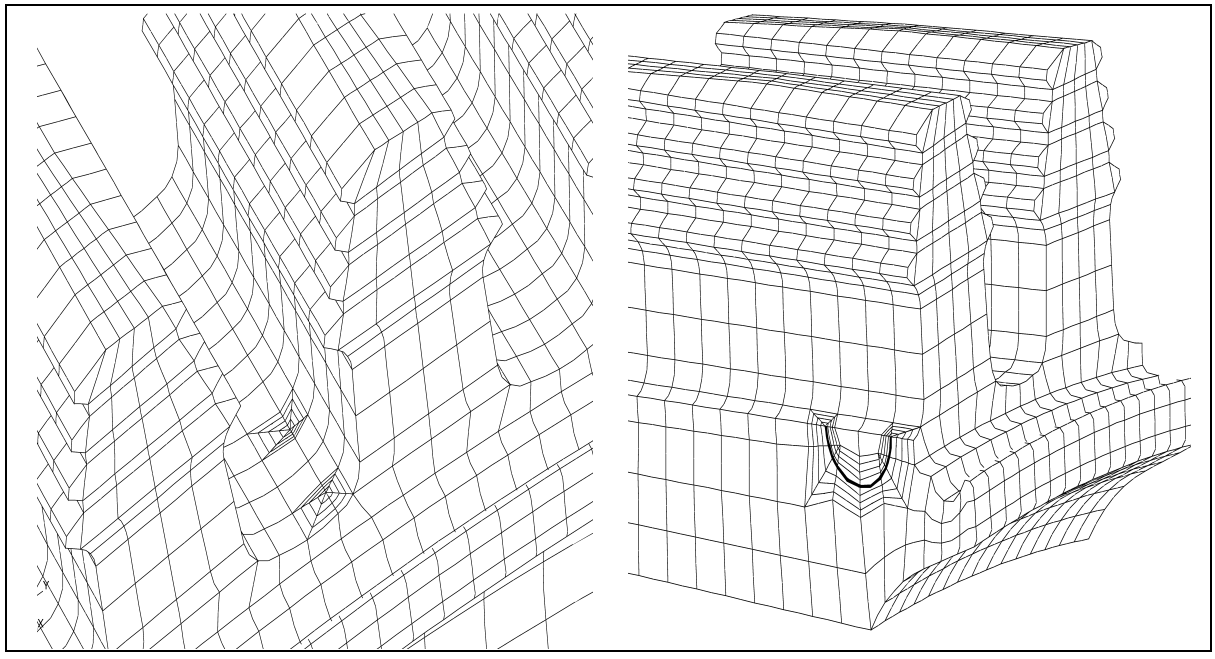

FIGURE 3 : CRACK GEOMETRY INTRODUCED INTO FE-MESH

3D FE Calculations under *reference load* conditions:

1) for the uncracked structure (linear-elastic and elastic-plastic)

2) with different crack sizes (linear-elastic)

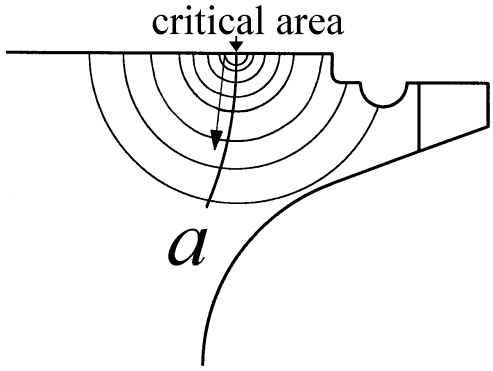

Result: *stresses* and *stress intensity factors* as a function of the chosen crack path a

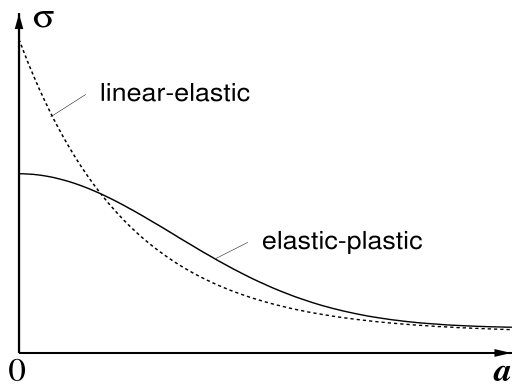

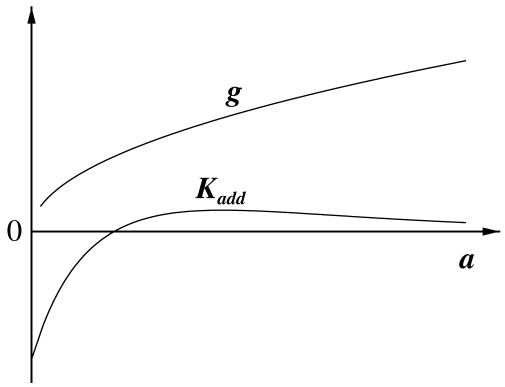

Representation of the stress intensity factor K as a function of the *monitored* elastic stress $\sigma_{critical\ area}$:

$$K(a) = g(a) \cdot \sigma_{critical\ area} + K_{add}(a)$$

Table installed in On-Board Life Monitoring System :

crack depth a	accumulated *reference cycles* N	geometry factor g	initial plastification correction term K_{add}	crack growth rate for *reference cycle* $(da/dN)_{ref}$
...	...	...	...	...
...	...	...	...	...
...	...	...	...	...

FIGURE 4: GENERATION OF DATA BASE TABLE USED FOR CRACK PROPAGATION MONITORING

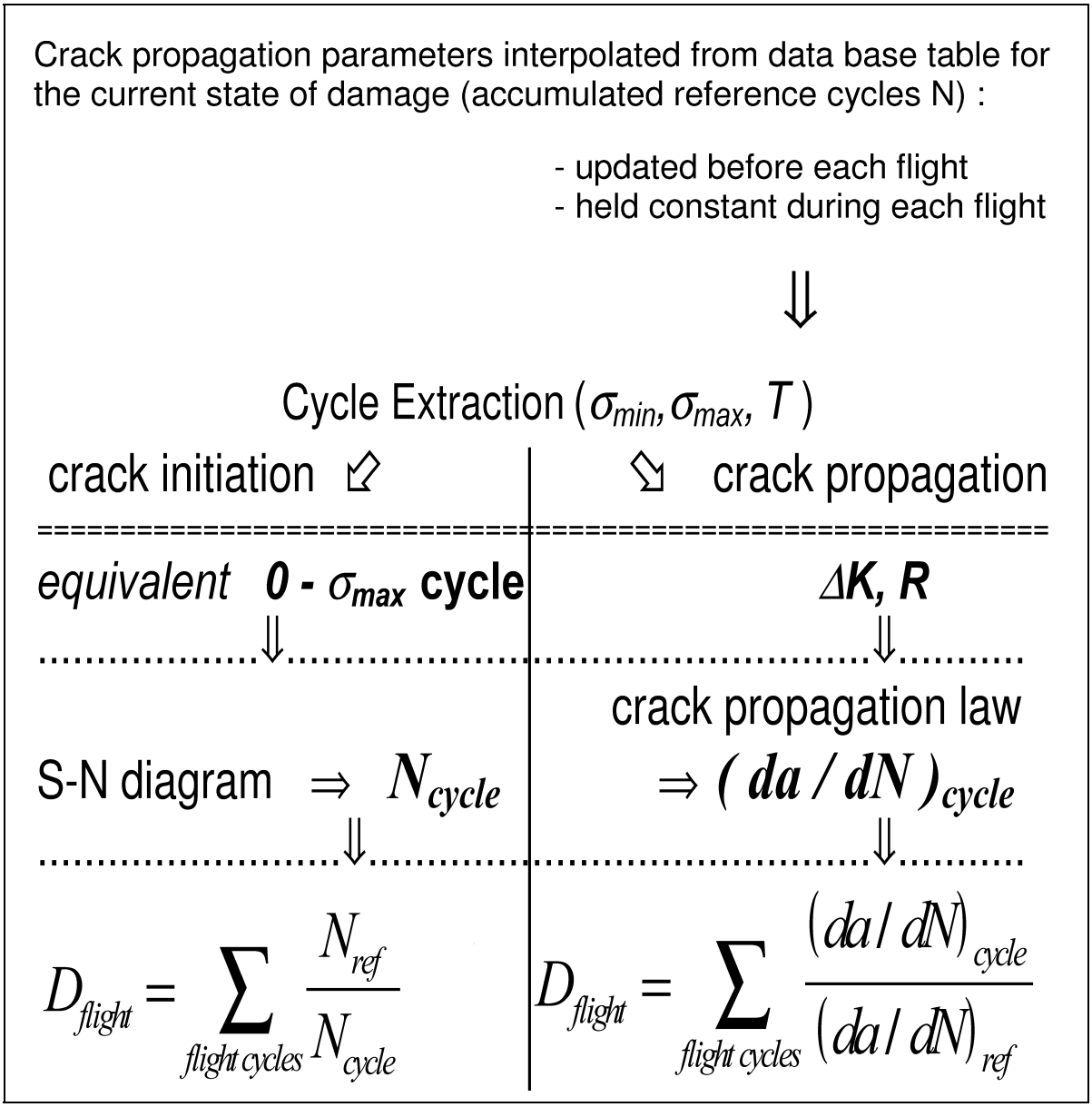

FIGURE 5 : FLIGHT DAMAGE CALCULATION SCHEME